Journal of Power Sources 312 (2016) 55–59

Contents lists available at ScienceDirect

Journal of Power Sources

journal homepage: www.elsevier.com/locate/jpowsour

Influence of memory effect on the state-of-charge estimation of large-format Li-ion batteries based on $LiFePO_4$ cathode

Wei Shi [a, b], Jiulin Wang [b, c], Jianming Zheng [b], Jiuchun Jiang [a], Vilayanur Viswanathan [b], Ji-Guang Zhang [b, *]

[a] National Active Distribution Network Technology Research Center, School of Electrical Engineering, Beijing Jiaotong University, No. 3 Shangyuancun Street, Beijing 100044, China
[b] Energy and Environment Directorate, Pacific Northwest National Laboratory, P.O. Box 999, Richland, WA 99352, USA
[c] School of Chemistry and Chemical Engineering, Shanghai Jiaotong University, No. 800 Dongchuan Road, Shanghai 200240, China

HIGHLIGHTS

- The memory effect in a $LiFePO_4$/graphite battery is more complex than in a half-cell.
- The memory effect is affected by the depth of discharge during the memory writing.
- The memory effect in large batteries is affected by parameter distribution.
- The memory effect needs to be considered in a battery management system.

ARTICLE INFO

Article history:
Received 9 October 2015
Received in revised form
4 January 2016
Accepted 11 February 2016
Available online xxx

Keywords:
$LiFePO_4$ battery
Memory effect
Partial charge
SOC
DOD

ABSTRACT

In this work, we systematically investigated the influence of the memory effect of $LiFePO_4$ cathodes in large-format full batteries. The electrochemical performance of the electrodes used in these batteries was also investigated separately in half-cells to reveal their intrinsic properties. We noticed that the memory effect of $LiFePO_4$/graphite cells depends not only on the maximum state of charge reached during the memory writing process, but is also affected by the depth of discharge reached during the memory writing process. In addition, the voltage deviation in a $LiFePO_4$/graphite full battery is more complex than in a $LiFePO_4$/Li half-cell, especially for a large-format battery, which exhibits a significant current variation in the region near its terminals. Therefore, the memory effect should be taken into account in advanced battery management systems to further extend the long-term cycling stabilities of Li-ion batteries using $LiFePO_4$ cathodes.

1. Introduction

The lithium (Li)-ion battery is one of the most promising energy storage systems used in large-scale energy storage applications such as pure electric vehicles (EVs) and plug-in hybrid electric vehicles (PHEVs), as well as grid applications [1–5]. To extend the lifespan of Li-ion batteries, advanced battery management systems (BMSs) have been widely used, especially for high energy/power-density applications. However, the success of Li-ion systems strongly depends on accurate determination of the state of charge (SOC), which has a closed relationship with cell voltages and estimation of battery performances. During the last a few decades, many complicated methods have been proposed for the accurate determination of cell voltage and SOC. These methods include the extended Kalman filter [6–8], the dual Kalman filter [9–11], nonlinear observers [12,13], the sliding-mode observer [14], fuzzy neural networks [15–17], and the reduced-order electrochemical model [18]. Generally, equivalent circuit models, including the first-order, second-order, or electrochemical equivalent models [19,20], were used to simulate the open-circuit voltage and terminal voltage, where terminal voltage is cell voltage under load or during charge. To date, $LiFePO_4$ cathode material has been widely used in energy storage systems including EV and large-scale stationary applications because of its excellent cycling performance, low cost, and environmentally benign properties. However, the very flat

* Corresponding author.
E-mail address: jiguang.zhang@pnnl.gov (J.-G. Zhang).

http://dx.doi.org/10.1016/j.jpowsour.2016.02.041
0378-7753/

voltage profile of $LiFePO_4$ makes it difficult to estimate the SOC with high accuracy. Although memory effect is one of the other factors that significantly affect estimation of the SOC in nickel cadmium batteries [21] and nickel metal hydride batteries [22], the absence of a memory effect has often been regarded as one of the advantages of Li-ion batteries.

Surprisingly, Sasaki et al. [23] reported recently that $LiFePO_4$ cathode material does exhibit a memory effect. After $LiFePO_4$ cathode was partially charged/fully discharged (so called "memory writing") process, the voltage profile during subsequent charge (so called "memory release") process exhibits positive deviation or a bump at the location corresponding to the SOC reached during the memory writing process. This deviation will lead to SOC estimation error. A multi-particle model based on the two-phase equilibrium (a Li-rich phase coexisting with a Li-poor phase) of the $LiFePO_4$ system was proposed by Sasaki et al. to explain the memory effect [23]. For a practical BMS, a slight voltage bump may not have significant effects on the SOC estimation of a cathode with a large voltage slope, but it will have remarkable effects on a cathode with a very flat voltage profile (such as $LiFePO_4$). Therefore, it is necessary to investigate how this newly discovered memory effect affects the management of full batteries used in practical applications.

In Sasaki's study [23], coin cells with a configuration of $LiFePO_4$/Li half-cells was used to study the memory effect in $LiFePO_4$. However, most commercial $LiFePO_4$ batteries used graphite as the anode. In this case, the influence of the memory effect of a $LiFePO_4$ cathode on the battery management becomes more complicated due to the multi-voltage plateau of graphite anodes (in contrast to the single voltage plateau of $Li_4Ti_5O_{12}$). Therefore, the primary challenge of determining the influence of the memory effect on commercial batteries is to distinguish the source of the voltage variation in $LiFePO_4$ batteries. The memory effect of $LiFePO_4$ was found to occur near the SOC value where the previous partial charge was terminated during the memory writing process. However, the values of voltage deviations vary significantly with the maximum SOC level reached during the memory writing process, thus increasing the uncertainty of SOC estimation in the next cycle.

In this work, we investigated the voltage fluctuation phenomenon at different SOCs and DODs using commercial $LiFePO_4$/graphite batteries. For clarity, we used SOC and depth of discharge (DOD) to represent the maximum SOC reached during the charge process and the maximum DOD reached during the discharge process of the memory writing step, respectively, unless specified otherwise. To improve the reliability of SOC estimation used in BMSs, the effect of the memory phenomena of $LiFePO_4$ cathode and the multi-stage voltage of graphite have been combined as the voltage bumps observed in the full batteries. The relationship between these voltage bumps and the amplitude of the voltage bumps in commercial $LiFePO_4$/graphite batteries was also identified.

2. Experimental

A 2 Ah battery (Model 26650, A123 Systems, LLC) with a $LiFePO_4$ cathode and a graphite anode was used to investigate the memory effect in a full battery. The battery was first fully charged/discharged between 2.5 V and 3.65 V using a battery testing system (Model BT-2000, Arbin Instruments), then partially charged/discharged to different SOC intervals. The $LiFePO_4$ cathode and graphite anode used in the $LiFePO_4$/Li and graphite/Li half-cell tests were obtained from a disassembled, as-received A123 battery. The dimensions of the electrode for the 26650 type A123 battery are 1.6 m (length) × 55 mm (width), and the dimensions of the tab are 10 mm (length) × 5 mm (width). The anode current collector (copper foil) is 7 μm thick, the cathode current collector (aluminum foil) is 13 μm thick, and the positive and negative electrodes each have four tabs. The 2032 coin-type half-cells were assembled in an argon filled glove box with oxygen and moisture levels of less than 1 ppm. Celgard 2045 was used as the separator and 1 M $LiPF_6$ in ethylene carbonate/dimethyl carbonate solution (volume ratio = 1:2) was used as the electrolyte. The reassembled half-cell was initially charged/discharged at a rate of C/10 for five cycles until a stable capacity was reached. The memory-writing and memory-release procedures were the same as those reported by Sasaki et al. [23]. In this process, a memory writing cycle is a partial charge/discharge process; a memory release cycle is a full charge/discharge process after a memory writing cycle. The rest time after partial charge was set at 1 h, the rest time between memory writing (including partial charge and rest) and memory releasing was set at 10 min, and a C/2 rate was used in all the tests unless specified otherwise.

3. Results and discussion

3.1. Positive and negative electrode matching

To identify the loading ratio of battery and Li-ion insertion/extraction regions in both electrodes, the half-cell and full-cell capacities were tested at 1 mA with 2032 coin-type cells. In the power type $LiFePO_4$/graphite battery investigated in this work, ~10% more cathode material has been used. Fig. 1 shows the initial voltage profiles of reassembled coin-type half cells and full cell using positive electrode ($LiFePO_4$), the negative electrode (graphite) obtained from a disassembled A123 commercial battery. As shown in Fig. 1, the $LiFePO_4$ (LFP) cathode shows slightly higher capacity than the graphite anode. It indicates that the battery investigated in this work has an areal specific capacity ratio of 1.2:1.1:1 for LFP:graphite:battery.

3.2. Memory effects at different SOCs and DODs

Fig. 2 shows the memory-effect testing profiles and voltage curves at different SOC levels for a 2 Ah $LiFePO_4$/graphite battery when the DOD was fixed at 100%. As shown in Fig. 2a, the memory writing (a partial charge/full-discharge process) and memory release (a full-charge/full-discharge process after a memory writing process) processes were carried out at different SOC ranges between 30% and 80%. Fig. 2b shows voltage deviation curves derived by subtracting the standard charging voltage from the charging

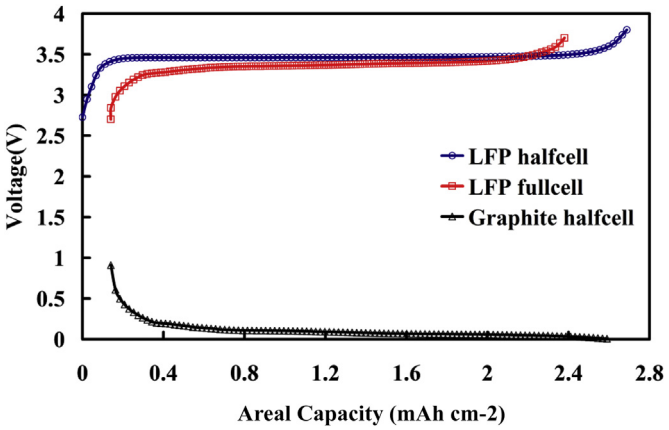

Fig. 1. Initial voltage curves of reassembled coin half-cells and full cell using electrodes [positive electrode ($LiFePO_4$), negative electrode (graphite)] from an A123 commercial battery.

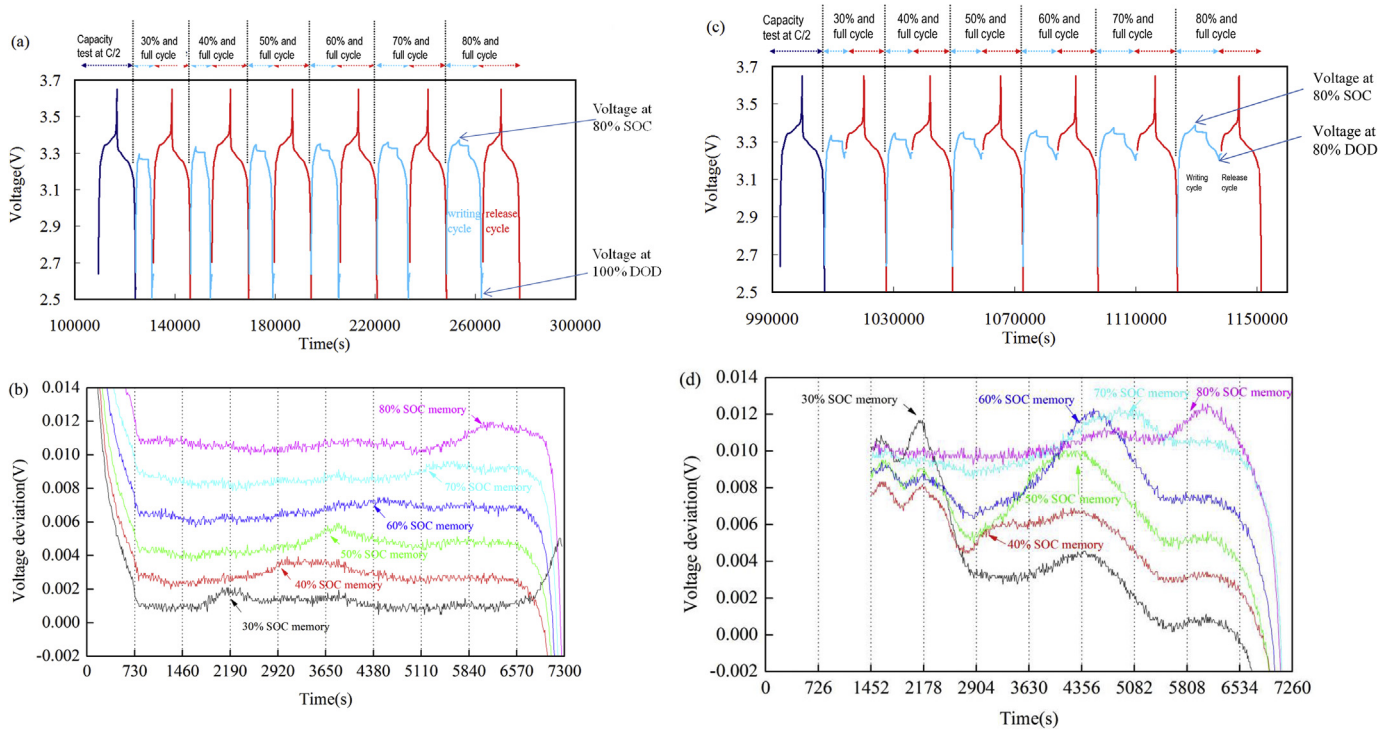

Fig. 2. Memory-effect testing and validation at different SOC intervals for a 2 Ah A123 $LiFePO_4$/graphite battery: (a) memory writing and release at different SOC intervals with 100% DOD; (b) degree of voltage deviation of (a); (c) memory writing and release at the different SOC intervals with 80% DOD; and (d) degree of voltage deviation of (c). Note: the deviation curves of (b) and (d) were shifted with a series constant voltage on the y-axis for easy comparison.

voltage curves of the memory release process (100% DOD). For easy comparison, the voltage deviation curves shown in Fig. 2b have been shifted upward along the y-axis by 2 mV for each 10% increase in SOC. The average voltage bump for a given SOC is about 1 mV.

It should be noticed that Li-ion batteries are typically discharged to 80% DOD rather than fully discharged in practical applications. Hence, the memory writing cycles was modified for selected 2 Ah cells to discharge to 80% DOD instead of 100% DOD in the memory writing cycle, after it was charged to a different SOC in the memory writing cycle. The memory writing/release profiles corresponding to 80% DOD are shown in Fig. 2c and the voltage deviations at different SOC intervals are shown in Fig. 2d. Similar to the case of Fig. 2b, the voltage variation curves shown in Fig. 2d have also been shifted upward along the Y-axis by 2 mV for each 10% increase in SOC. The voltage deviation curves during the voltage release cycles exhibit a much larger deviations when the battery was discharged to 80% DOD (see Fig. 2c) compared to those discharged to 100% DOD (see Fig. 2b) in the memory writing cycles. These results can be attributed to the memory writing profile when the $LiFePO_4$ electrode is not fully discharged during the previous memory writing cycle. These voltage deviations shown in Fig. 2d can lead to significant miscalculation when estimating the SOC of $LiFePO_4$ batteries by referring to the terminal voltages. Meanwhile, the multiple voltage plateaus of graphite anode materials make it more difficult to analyze the relationships between the amplitudes of voltage bumps and the positions of these bumps. Fig. 2d shows that the charge voltages during memory release process increase 10 mV, 6 mV and 2 mV when $LiFePO_4$/graphite battery was charged to 30%, 50%, and 80% SOC (corresponding to three plateaus of graphite anode), respectively while discharged to 80% DOD during memory writing process.

To eliminate interference produced by the graphite anode, the $LiFePO_4$ positive electrodes recovered from a disassembled A123 26650 battery were used to prepare a $LiFePO_4$/Li 2032 coin-type half-cell to further investigate the memory effect. The testing results of these half-cells are shown in Fig. 3. Fig. 3a and b show voltage curves and memory effects at different SOC during the previous memory writing process for a $LiFePO_4$/Li half-cell when it

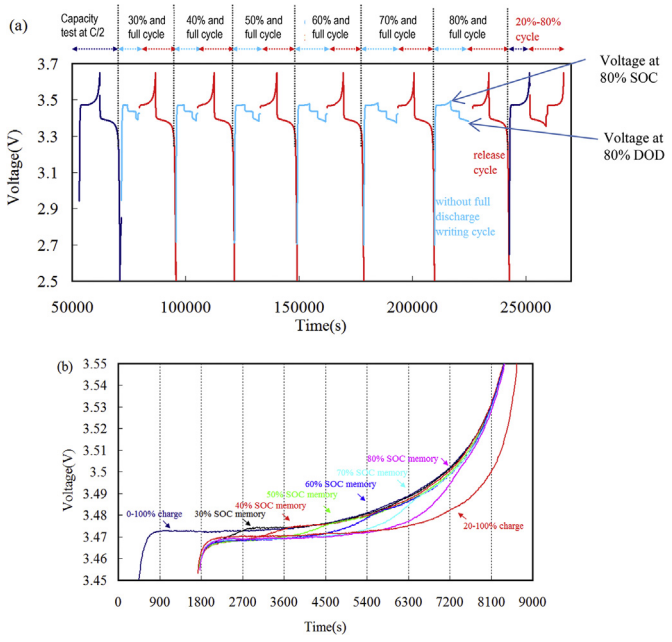

Fig. 3. Memory-effect testing and validation for different SOC ranges in a $LiFePO_4$/Li half-cell: (a) memory writing and release at the different SOC intervals with 80% DOD during memory writing cycle; (b) the degrees of voltage deviation of the different partial memory writing and release processes.

is only discharged to 80% DOD during the memory writing process. The cell exhibits obvious voltage deviations if it is charged to different SOCs during the memory writing processes. The memory effect of the material leads to an abrupt increase on the charging voltage curve at the SOC point of the previous memory writing cycle, which overlaps the charging voltage curves in a full charge/discharge process, as shown in Fig. 3b. In this case, the observed voltage bumps in the memory release cycles when they are discharged to 80% DOD seem to be jumping from 20–100% charge curve to 0–100% charge curve.

3.3. Internal parameter variation and memory effect

Based on memory-effect generation mechanisms [23], the $LiFePO_4$ voltage deviation mainly derives from the microstructure of the electrode material and the Li-ion diffusion limitation. In commercial batteries, the internal parameter distribution shows significant disparities, such as non-uniform voltage distribution and current distribution in different areas of large electrodes, because of a nonzero resistance in the electrodes. In contrast, the internal parameters of small coin cells reassembled with similar electrodes could be considered uniform. Generally, the terminal voltage of commercial batteries is measured near the battery tab, and the voltage in other parts of an electrode is undetectable by BMSs. As a result, it is difficult for BMSs to manage the instantaneous external characteristics of batteries properly because the terminal voltage values used in its equivalent circuit mode do not reflect the voltage deviations related to unequal internal parameter distributions. In addition to the space variation, the time variation of the voltages related to the voltage distribution and current distribution also affects the accurate determination.

To investigate the impacts of memory effect on the electrodes, two regions (including the cases of 30% and 50% SOC during the memory writing cycle) where the voltage deviations are prominent as discussed above were further analyzed. The results of voltage deviation for the $LiFePO_4$ materials in a half-cell charged to 30% and 50% SOC during the memory writing process are derived from Fig. 3b. The voltage deviations for the 2 Ah full batteries charged to 30% and 50% SOC during the memory writing process are shown in Fig. 2d. In both cases, batteries were discharged to 80% DOD during the discharge of the memory writing process. Fig. 4a and b compare the voltage deviations during the memory release cycle in the half-cells and full cells when the batteries were charged to 30% SOC (Fig. 4a) and 50% SOC (Fig. 4b) during the memory writing cycle. Taking into consideration that the 2 Ah battery investigated in this work has an initial area specific capacity ratio of 1.2:1.1:1 (see Fig. 1) for the positive electrode, negative electrode, and the full cell, the SOC values shown in Fig. 4 have been adjusted to reflect the actual SOC windows of the $LiFePO_4$/Li half-cell and the $LiFePO_4$/graphite full cell.

For the $LiFePO_4$/Li half-cell, different electrode regions on the 2032 coin-type electrode have relatively even SOC distributions because of the small size and flat voltage. However, for the 2 Ah $LiFePO_4$/graphite battery with large electrode area, the potential gradient across the electrode leads to a more uneven SOC distribution, which may result in different memory effect and voltage deviation at different locations of the electrode. In addition, the voltage plateaus and the phase change of the graphite anode also affect the polarization state and voltage of the full battery at different SOCs. These differences reveal why the full-cell voltage deviation curves are different from the voltage deviation profile of the half-cell.

In an effort to incorporate the memory effect into a BMS to give a more accurate estimate of the voltage/current distribution in a large-format battery, the internal parameters have been calculated

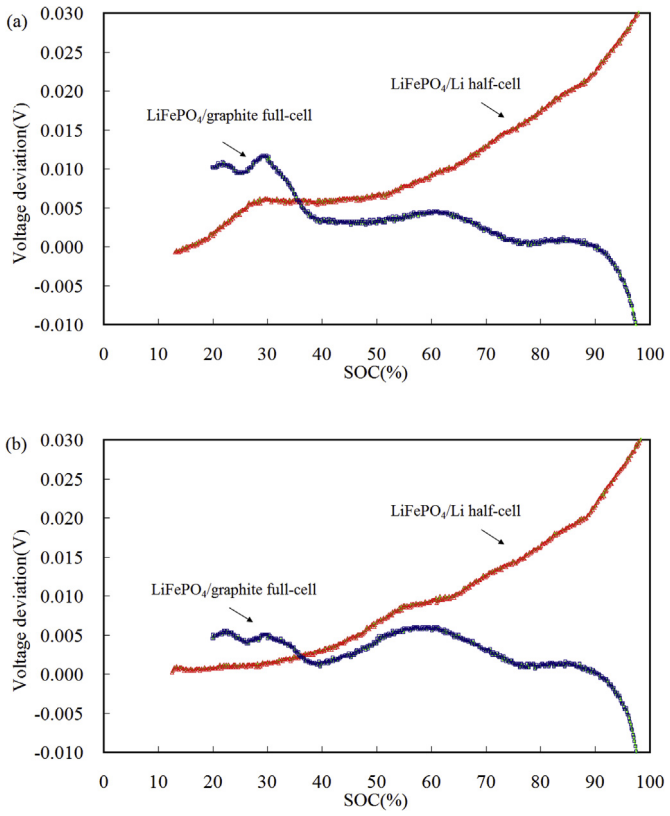

Fig. 4. Memory-effect voltage deviation curves for the $LiFePO_4$/Li half-cell and the $LiFePO_4$/graphite full cell when the batteries were charged to (a) 30% SOC and (b) 50% SOC during the memory writing cycle.

based on previously reported models [24–26]. The current changes at electrodes of a 2 Ah battery at two typical positions (near to and far from the tabs) and the SOC variations with and without memory effects were simulated, assuming the batteries were charged to 50% SOC in the previous cycle. In this case, the memory writing process for the 50% SOC starts at 0% SOC and continues until an SOC of 50% is reached, which is followed by discharging to reach an 80% DOD. By overlaying the 20% SOC the memory-release charging curve on the $LiFePO_4$/Li half-cell's voltage deviation curve (shown in Fig. 3b), the full cell's electrode voltages and its imbalanced currents can be simulated. For convenience, the overlaid voltage bump

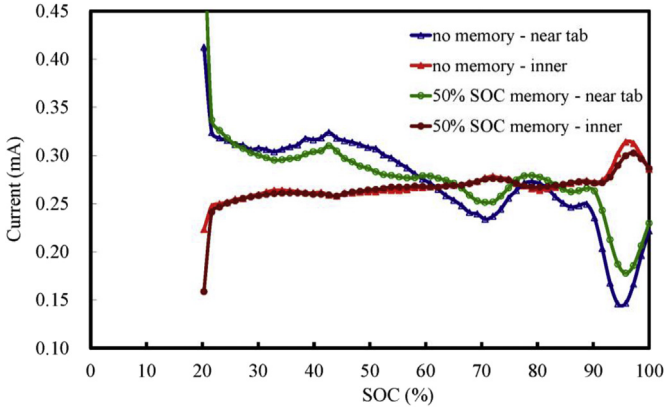

Fig. 5. Imbalanced current curves near to and far from the tab for the processes without and with memory effects when batteries were charged to 50% SOC in the previous cycle.

phenomenon of the full battery was converted to an increased battery polarization resistance. Furthermore, the simulation curves in different regions near to and far from the tabs were obtained, and the current curves with and without memory effects for a fullcell are shown in Fig. 5. It is clear that the currents of the grids near the tab with 20% SOC at the initial charging level are much greater than those far from the tab. As a consequence, the electrode currents near the tab are much smaller than those far from the tab at the end of charging. Moreover, as a result of the memory effect at around 50% SOC, current density in the regions near the tab is reduced. The unbalanced current can be attributed to the SOC differences in different regions of the battery during the charging process. The voltage deviation that results from memory effects occurs at SOC values reached in the previous cycle. Due to the larger current density at the initial charging stage, the regions near the tab are affected by the memory effect earlier, which then changes the current, voltage, and SOC variation trends during the subsequent charging process. Consequently, the obvious uneven distribution of internal parameter in a practical full battery further complicates the implications of the memory effect of the $LiFePO_4$ cathode on operation of the full cell. Therefore, an advanced BMS should take into account both the physical dimensions of the electrode and the memory effect to accurately estimate the SOC for Li-ion batteries with $LiFePO_4$ cathode materials.

4. Conclusions

The memory effect of $LiFePO_4$ may affect the accurate measurement of SOC in a $LiFePO_4$/graphite battery, which should be considered in the operation of BMSs. In this study, we found a complicated memory effect in the voltage curve of a large-format battery, and noticed that the memory effect becomes more prominent if the battery was discharged to 80% DOD during the memory writing process (this is the more common case in practical applications) compared to those discharged to 100% DOD. Experimental results further indicate that the memory effect in $LiFePO_4$ cathode materials clearly affects terminal voltage, leading to a variation and miscalculation of SOC estimations. In addition, this voltage bump phenomenon is more complex for $LiFePO_4$/graphite practical batteries than for a $LiFePO_4$/Li half-cell. Moreover, in a large-format battery, the SOC in different regions of the battery may vary because of the variations of internal current density in the battery. As a result, the memory effect in different regions of the battery may be different. Consideration of the memory effect in BMS systems can increase the accuracy of battery voltage estimation and further enhance the reliability of BMSs for batteries using $LiFePO_4$ cathode materials.

Acknowledgments

This work was supported by the Assistant Secretary for Energy Efficiency and Renewable Energy, Office of Vehicle Technologies of the U.S. Department of Energy under the Advanced Battery Materials Research Program (Contract No. DE-AC02-05CH11231, Subcontract No. 18769) and by the Fundamental Research Funds for the Central Universities of China (Grant Number E15JB00050), and the Power Electronics Science and Education Development Program of Delta Environmental & Educational Foundation.

References

[1] G. Ceder, Y.M. Chiang, D.R. Sadoway, M.K. Aydinol, Y.I. Jang, B. Huang, Nature 392 (1998) 694–696.
[2] J.M. Tarascon, M. Armand, Nature 414 (2001) 359–367.
[3] Y.-M. Chiang, Science 330 (2010) 1485–1486.
[4] J.M. Zheng, X.B. Wu, Y. Yang, Electrochim. Acta 56 (2011) 3071.
[5] J. Zheng, M. Gu, J. Xiao, P. Zuo, C. Wang, J.-G. Zhang, Nano Lett. 13 (2013) 3824.
[6] G.L. Plett, J. Power Sources 134 (2004) 252–261.
[7] G.L. Plett, J. Power Sources 134 (2004) 262–276.
[8] G.L. Plett, J. Power Sources 134 (2004) 277–292.
[9] J. Kim, S. Lee, B.H. Cho, IEEE Trans. Power Electron. 27 (2012) 436–451.
[10] J. Kim, B.H. Cho, IEEE Trans. Energy Convers. 28 (2013) 1–11.
[11] D. Andre, C. Appel, T. Soczka-Guth, D.U. Sauer, J. Power Sources 224 (2013) 20–27.
[12] C. Hametner, S. Jakubek, J. Power Sources 238 (2013) 413–421.
[13] B.S. Bhangu, P. Bentley, D.A. Stone, C.M. Bingham, IEEE Trans. Veh. Technol. 54 (2005) 783–794.
[14] I.-S. Kim, J. Power Sources 163 (2006) 584–590.
[15] M. Charkhgard, M. Farrokhi, IEEE Trans. Indus. Electron. 57 (2010) 4178–4187.
[16] B. Cheng, Z. Bai, B. Cao, Energy Convers. Manag. 49 (2008) 2788–2794.
[17] H. He, R. Xiong, J. Fan, Energies 4 (2011) 582–598.
[18] J. Marcicki, M. Canova, A.T. Conlisk, G. Rizzoni, J. Power Sources 237 (2013) 310–324.
[19] B.Y. Liaw, G. Nagasubramanian, R.G. Jungst, D.H. Doughty, Solid State Ionics 175 (2004) 835–839.
[20] M. Dubarry, B.Y. Liaw, J. Power Sources 174 (2007) 856–860.
[21] Y. Sato, K. Ito, T. Arakawa, K. Kobayakawa, J. Electrochem. Soc. 143 (1996) L225.
[22] M. Morishita, S. Shikimori, Y. Shimizu, A. Imasato, H. Nakamura, K. Kobayakawa, Y. Sato, Electrochemistry 74 (2006) 532.
[23] T. Sasaki, Y. Ukyo, P. Novak, Nat. Mater. 12 (2013) 569–575.
[24] U.S. Kim, C.B. Shin, C.-S. Kim, J. Power Sources 189 (2009) 841–846.
[25] M. Fleckenstein, O. Bohlen, M.A. Roscher, B. Baeker, J. Power Sources 196 (2011) 4769–4778.
[26] G.-H. Kim, K. Smith, K.-J. Lee, S. Santhanagopalan, A. Pesaran, J. Electrochem. Soc. 158 (2011) A955–A969.